Construction and Building Materials 199 (2019) 483–491

Contents lists available at ScienceDirect

Construction and Building Materials

journal homepage: www.elsevier.com/locate/conbuildmat

# Damage progression analysis in a historical timber framed wall under cyclic loads through an image-based tracking method

Jakub Sandak [a,b,c,*], Mariapaola Riggio [d], Nicola Ruggieri [e], Anna Sandak [a,b,c]

[a] Trees and Timber Institute, CNR-IVALSA, via Biasi 75, 38010 San Michele all'Adige, Italy
[b] InnoRenew CoE, Livade 6, 6310 Izola, Slovenia
[c] University of Primorska, Andrej Marušič Institute, Muzejski trg 2, 6000 Koper, Slovenia
[d] Oregon State University, Department of Wood Science & Engineering, 236 Richardson Hall, Corvallis, OR 97331, USA
[e] Soprintendenza archeologia belle arti e paesaggio per le province di Catanzaro Cosenza e Crotone, Piazza Valdesi, 14, 87100 Cosenza, Italy

## HIGHLIGHTS

- Historical timber-framed wall system was investigated under cyclic loads.
- Damage progression and post-elastic behaviour was analysed by image-based tracking method.
- Plastic deformations and local damage occurred in some joints.
- Observations are important for the design of strengthening or repair interventions.

## ARTICLE INFO

*Article history:*
Received 23 May 2018
Received in revised form 28 October 2018
Accepted 10 December 2018

*Keywords:*
Image-based tracking
Cyclic loads
Damage progression
Historical timber-framed wall

## ABSTRACT

The scope of this paper is to analyse local phenomena associated with the damage progression and post-elastic behaviour of a historical timber-framed wall system under cyclic loads. It was assessed on series of points identified on the wall by processing time-resolved sequences of images. Dedicated methodology of image-based tracking method was developed to analyse local phenomena, such as relative displacements, rotations and deformations in the wall. It was possible to deduce that plastic deformations and local damage occurred in some joints. This type of observation is important for the design of rigorous strengthening or repair interventions.



## 1. Introduction

The scope of this paper is to analyse local phenomena associated with the damage progression and post-elastic behaviour of a historical timber-framed wall system under cyclic loads. The Borbone construction system, also known as *casa baraccata*, developed after the earthquake that hit the south of Italy in 1783 uses masonry reinforced with timber frames. It is an implementation of an initial approach to seismic design standards during the 18th century [1]. The Borbone standard prescribed the use of a timber skeleton to reinforce a masonry wall and to connect corner walls to obtain a box-like behavior as a requirement for the reconstruction of aseismic buildings.

In cases of repeatedly applied loads, such as seismic conditions, failure generally results from damage accumulation and a gradual degradation of the mechanical properties of the materials. This damage is characterized by the increasing amplitude of repeated horizontal actions. The present study aimed to elucidate local phenomena and kinematics of damage on an isolated component of the Borbone system, complementing findings of past research of Authors reporting damage of actual buildings in Calabria (Italy) [2,3]. They analysed primary sources (photographs and post-event reports) documenting the conditions of ten *case baraccate* after the earthquakes that hit Calabria in 1905 (moment magnitude of 7.2 Mw and Intensity MCS XI) and 1908 (7.1 Mw, MCS XI). From the analysed sources, two main types of damage were observed in most cases: local expulsion of the masonry infill and out-of-plane collapse of the upper part of a façade, caused by unrestrained thrusts of the roof trusses. Accurate assessment of damage

* Corresponding author at: InnoRenew CoE, Livade 6, 6310 Izola, Slovenia.
*E-mail addresses:* jakub.sandak@innorenew.eu (J. Sandak), mariapaola.riggio@oregonstate.edu (M. Riggio), nicola.ruggieri@beniculturali.it (N. Ruggieri), anna.sandak@innorenew.eu (A. Sandak).

https://doi.org/10.1016/j.conbuildmat.2018.12.044
0950-0618/

levels and mechanisms in the studied timber framed masonry system is a necessary step toward the definition of appropriate repair and strengthening actions for this type of historical system. As a general principle, designing interventions should ensure that in case of high stresses ruptures and deformations will occur at new, dissipative elements. It defines a hierarchy of failure mechanisms, maximizes structural performance and minimizes loss of the heritage system.

A novel methodology has been developed to analyse local phenomena, such as relative displacements, rotations and deformations in the wall, occurring during cyclic loading. The methodology uses time-laps images extracted from video frames of the wall at different loading stages. The advantages and limitations of the proposed experimental approach are also discussed.

## 2. Characterization of historical timber framed systems: overview

Studies on the seismic response of timber structures are mainly concentrated on modern systems. Only recently, a few researchers have studied the seismic behaviour of historical timber frames. There is still insufficient knowledge and scarce scientific literature on the damage progression of traditional timber framed structures, such as the Borbone system, which are typical in earthquake-prone areas.

The Portuguese *Gaiola*, used for the reconstruction of Lisbon after an earthquake in 1755, has been the object of numerous studies. The first cyclic tests on a Gaiola panel were performed on a real wall specimen extracted from an existing building [4]. Gaiola walls have been tested with different frame infills, and in dynamic tests on strengthened and non-strengthened prototypes on a 3D shaking table [5]. Unreinforced timber frame units have been compared against frames with joints strengthened by mechanical connectors [6]. Several samples with different types of joints: cross-halved, mortise-tenon with a timber dowel, mortise-tenon with "L" shaped metal plates, mortise-tenon with "T" shaped metal plates, and mortise-tenon with hold-down, have been tested under the CUREE loading protocol [7] in the laboratories of Tokyo Institute of Technology [8], in order to assess the influence of the different connection types in the behaviour of the Gaiola system. In all the above cited experimental campaigns, cumulative damage appeared in the Gaiola system and was mainly concentrated in the joints, highlighted by plastic deformations and ruptures [4–8]. In particular, from the first displacements tension diagonals experienced a detachment and, with load direction variation the compressed bracings were characterized by a rupture at the intermediate connections preceded by the buckling of the member.

Quasi-static cyclic tests, followed by a shaking table test, were conducted to better understand the *Dhajji Dewari* behaviour under cyclic loading [9]. The study highlighted a predominant role of the timber frame with no contribution from the infill in the horizontal loads withstanding.

The behaviour differed from in-plane cycle tests on traditional *Quincha* [10], a distinct Peruvian timber frame wall. In fact, the tested samples in a 1:2 scale showed a significant contribution of the infill of mud and cane in increasing stiffness of the frame.

Aktas et al. [11] investigated the cyclic behaviour of a *Himis* wall, the traditional Ottoman wooden framed wall. The studies were carried out on timber frames with and without adobe infill considering different timber frame geometries as well as the presence of openings. The tests showed that damage was governed by joint behaviour and gave important data on the load bearing capacity of this type of timber frame.

Ceccotti et al. conducted a study on a masonry wall reinforced with a timber frame typical of the rural architecture in the Italian Dolomites area [12]. The experimental study showed the strategic roles on the seismic behaviour of both, the degree of anchorage and interaction between the timber frame and the masonry infill of the compound system.

An experimental program, including monotonic, cyclic and shaking table testing, was carried out at the Mechanical Laboratory of the French Institute FCBA on Haitian timbered masonry structures called *Kay peyi* [13]. The study included tests of components at the different scales: the joint, an elementary frame, a shear wall and an entire house. The latter was tested on shaking table and submitted to a ground motion equivalent to the January 12th 2010 Haiti earthquake and showed the proper behaviour, recording no damage. A digital image correlation (DIC) analysis of a full-scale wall under seismic loading applied by a shake table was included in that study. The DIC measurements, using the open source software Tracker, showed a perfect correspondence between the shaking table displacement recorded by LVDT and that obtained by DIC technique.

The study presented in the following sections is based on cyclic tests on a timber-reinforced masonry wall, representing a full-scale reproduction of a wall built according to the Borbone anti-seismic provisions. This study includes data obtained with an original image-based tracking method for the evaluation of damage progression.

## 3. Material and methods

### 3.1. Specimen configuration

The tested wall was a replica of a timber framed wall in the "*Palazzo del Vescovo*" (Bishop's Palace) in Mileto, Italy (Fig. 1). The Palace was built at the end of the 18th century and showed a good performance during the earthquake in 1908, as reported by a contemporary inspection report [14]. The masonry wall was constituted by roughly squared calcilitute stone blocks mixed with wedge bricks, laid with a hydraulic mortar. The bed joint mortar was about 2–3 cm thick and was composed of lime and quartz-granitic aggregate with dimensions between 2 and 5 mm. The wall was reinforced by a timber frame without cross bracing, placed at the internal part of the masonry. The wooden members, made of Calabrian Chestnut (*Castanea sativa Mill.*), were posts ($12 \times 12$ cm$^2$ cross section) running from the top plate ($13 \times 14$ cm$^2$), to the sill plate ($12 \times 12$ cm$^2$). Other horizontal timbers with a square section varying from $10 \times 10$ cm$^2$ to $12 \times 12$ cm$^2$ were encapsulated in the masonry and connected to the posts using half-lap joints. The entire wall section measured 339 cm in length, 295 cm in height and was 41 cm thick. The carpentry joints were manufactured to reproduce the gaps between contact faces similar to the original handcrafted connections. The joints in the tested frame were reinforced with pyramid-forged nails with maximum cross section of 10 mm. These fasteners replicated the typical pre-industrial wrought iron nails and were driven from the back side of the frame. Mechanical properties of materials used for construction of the replica wall were: MOR = 10 MPa and compression strength = 124 MPa for Trentino limestone [15], MOR = 48 MPa and MOE = 13,000 MPa for Calabrian Chestnut [16] and yield strength = 154–247 MPa and tensile strength = 234–399 MPa for wrought Iron [17].

### 3.2. Test setup and instrumentation

The test setup is presented in Fig. 2. The displacement was applied at the top of the wall by a piston-type hydraulic actuator with a ±500 kN capacity and a 500 mm stroke. According to the test protocol, both pushing (positive sign) and pulling (negative sign) were applied.

The bottom plate of timber frame was fixed to a 3-ply CLT panel (thickness 100 mm) using inclined self-tapping screws to connect the specimen to the lab floor. The CLT panel was connected to a steel beam fixed to the laboratory floor. The aim was to reproduce a stiff restraint and counteract both shear and tension (uplift) actions.

The upper part of the testing apparatus utilised lateral rollers to stabilise the top plate of the wall from buckling. A uniformly distributed vertical load (18.6 kN/m) was applied to the specimen by means of 4 hydraulic jacks to reproduce the actual loading conditions, i.e., the permanent gravity loads transmitted by the roof. Vertical loading was defined according to the Eurocode 1 [18], including only the self-weight of the structural and non-structural elements of the roof. Values of relative air humidity (65 ± 5%) and temperature (20 ± 2 °C) were measured during the test. The locations of the linear variable displacement transducers (LVDT) are indicated in Fig. 2 (whole wall diagonal, single frame diagonal, midpoint of the upper part of the wall, base and close to the actuator).

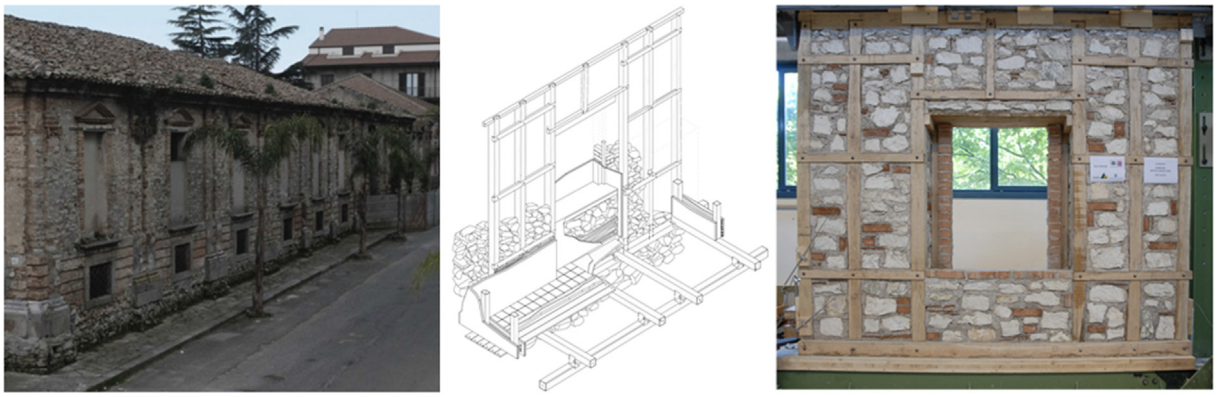

**Fig. 1.** Bishop's Palace, Mileto (Italy) (left), isometric view of the external wall (centre), tested replica wall (right).

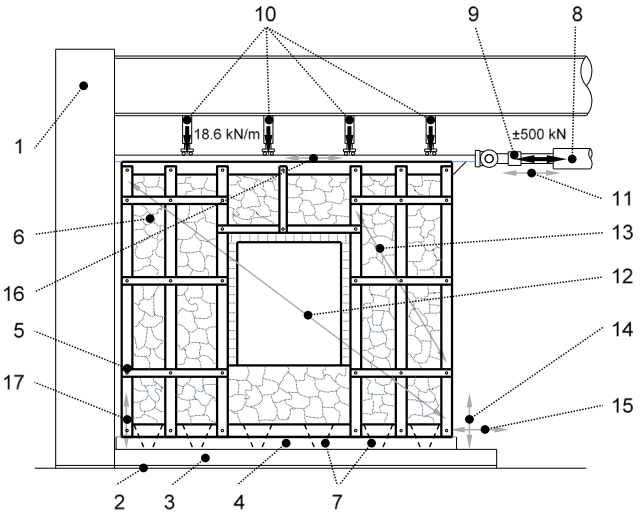


**Fig. 2.** Experimental setup: mechanical testing machine (1), floor (2), metal frame (3), cross-laminated timber foundation (4), wooden frame (5), masonry in-fill (6), metal fasteners (7), piston-type hydraulic cylinder (8), load cell (9), hydraulic jacks (10), displacement transducers (11–17).

### 3.3. Loading protocol

The cyclic test was performed adopting the procedures specified in the EN 12512:2006 standard [19]. This loading protocol provides the requisite information to define the ductility of the wall, as requested in the Eurocode 8 [20]. The test was carried out under displacement control, taking into account three constant amplitudes and completely reversed displacements (2.5, 5, 7, 10, 20 40, 60, 80 mm) corresponding to multiples and divisors of the estimated yielding displacement (EYD, 10 mm). The EYD was based on values recorded on similar construction systems and load history [21].

The cycles were conducted at a constant displacement rate of 0.2 mm/s. The last cycle was interrupted during pushing, thus affecting the reading of the residual values of strain, rotation and detachment, as highlighted in the conclusion section.

### 3.4. "Virtual transducers": application of an image-based tracking method

Complementary to the measurements taken by the LVDTs, local phenomena were assessed on series of points identified on the wall by processing time-resolved sequences of images. For that reason, colour images of the tested wall were acquired with a digital single lens reflex camera (Nikon D200) installed on the tripod in front of the structure with the optical axis direction perpendicular to the wall plane. The acquired image covered the overall area of the timber frame and mechanical testing machine. The camera was equipped with a 10.92 megapixels APS-C CCD sensor and a 16 mm lens (corresponding to 24 mm equivalent focal length) with f/5.6 aperture. Photographs were acquired every 3 s during loading with a shutter exposure time of 0.25 s. The image size was 2896 × 1944 pixels, resulting in a spatial resolution of 1.81 mm/pixel. The RGB colour image was converted to 8-bit grey scale by extracting the Luminance plane from the HSL image representation.

Custom software for pre-processing and analysis of the acquired images was developed in LabView 2016 (National Instruments, USA). Image and lens distortion corrections were performed before analysis by implementing a point coordinates calibration tool. The numerical tool applied for tracking the objects on the image was IMAQ_Find_Pattern_4 that bases on the pyramidal matching algorithm. The algorithm uses normalized cross-correlation and consists of two stages: learning and matching. It extracts grey value and/or edge gradient information from the source image during the first (learning) stage. Afterward, the pattern matching procedure extracts part of the searched image and locates regions with highest cross-correlation values. In this research, a manually selected Region-of-Interest (ROI) was extracted from the wall image before deformation. In the following step, the ROI position was matched on the rectangular search area defined on the corresponding wall image after deformation. The results of this search are both, a score (cross-correlation coefficient) and coordinates of the best corresponding ROI within the fitting rectangle. The score indicates similarity between the sought ROI and the detected region. The grayscale value pyramid numerical algorithm allows sub-pixel determination of the best corresponding ROI coordinates, thus increasing reliability of analysis and allowing detection of minor displacements. It is important to properly select points of interest *P* to assure some unique variance within the ROI image (i.e., high-contrast irregular patterns) and therefore increase the similarity score between sought and identified ROIs. Fig. 3 illustrates the principle of the "virtual transducers" method implemented here, where the width of the opening between the timber frame and mortise is identified. The size of the ROI implemented in this research is 11x11 pixels. It is possible to increase the analysis speed by limiting the search area of the ROI. For this reason, only a part of the investigated image is measured minimizing the number of computational operations and consequently CPU time.

The coordinates of *P* may later be used for computation of the geometric characteristics of the wall as deformation progresses. In this study, two, three and four points *P* were used for determination of the distances, rotations or strains respectively. This is schematically presented in Fig. 4 where locations of the most repre-

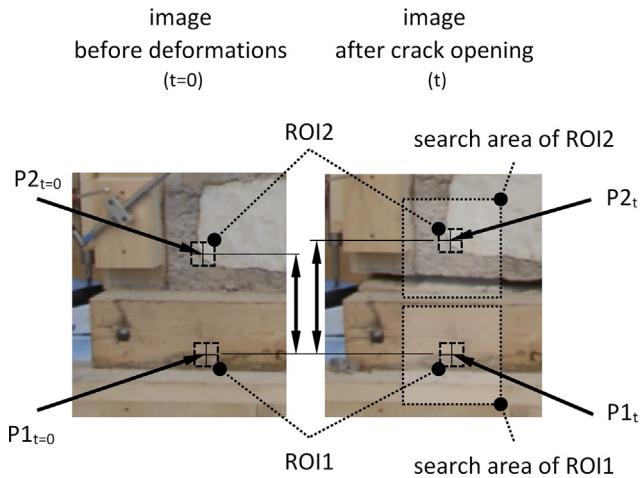


**Fig. 3.** Principle of the "virtual transducer" determining crack width after stress test: ROI – regions of interest corresponding to parts of image possessing unique pattern, P – coordinates of points corresponding to the centre of ROI, search area of ROI - the selected part of image where best fitting position of ROI is searched.

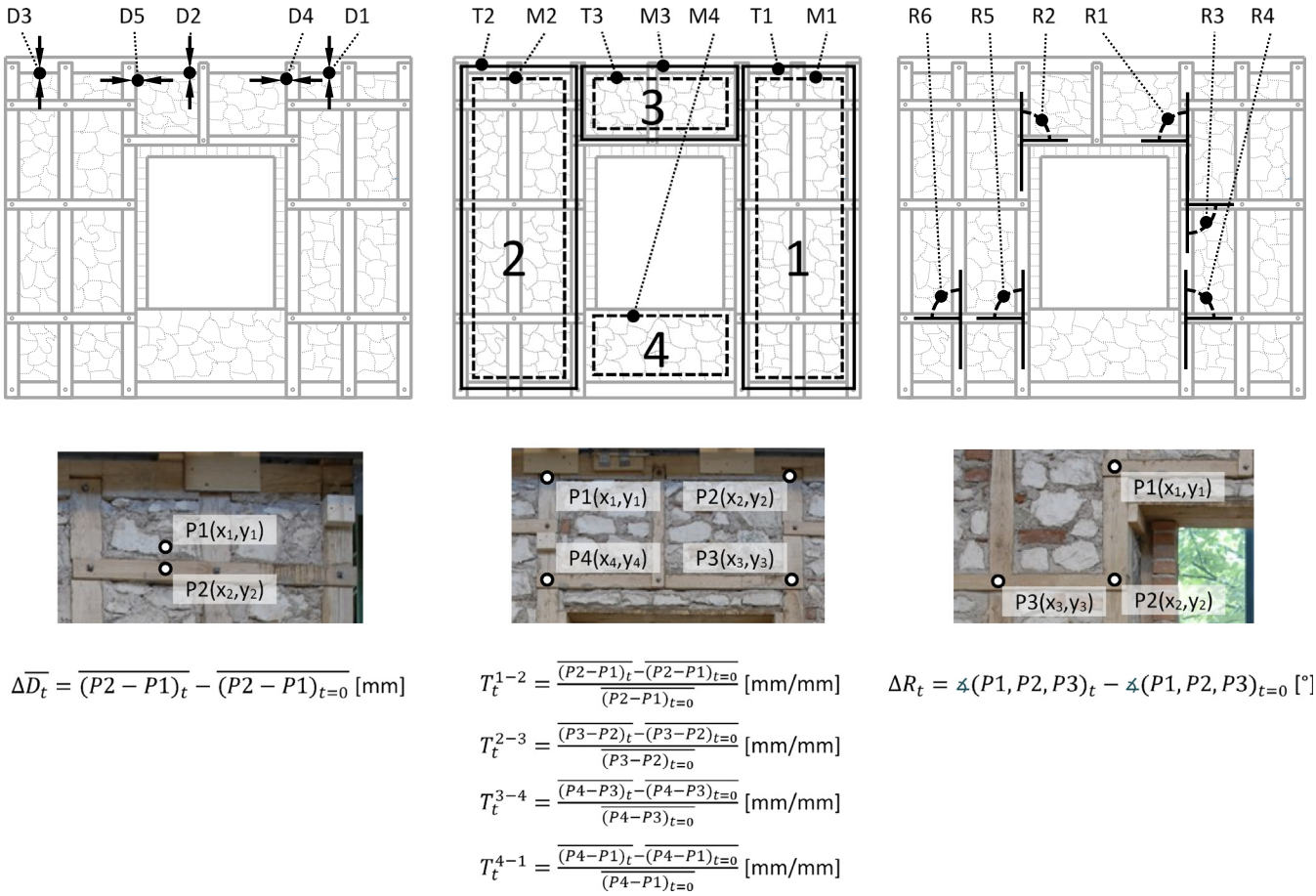


$$\Delta\overline{D_t} = \overline{(P2-P1)_t} - \overline{(P2-P1)_{t=0}}\ [\text{mm}]$$

$$T_t^{1-2} = \frac{\overline{(P2-P1)_t} - \overline{(P2-P1)_{t=0}}}{\overline{(P2-P1)_{t=0}}}\ [\text{mm/mm}]$$

$$T_t^{2-3} = \frac{\overline{(P3-P2)_t} - \overline{(P3-P2)_{t=0}}}{\overline{(P3-P2)_{t=0}}}\ [\text{mm/mm}]$$

$$T_t^{3-4} = \frac{\overline{(P4-P3)_t} - \overline{(P4-P3)_{t=0}}}{\overline{(P4-P3)_{t=0}}}\ [\text{mm/mm}]$$

$$T_t^{4-1} = \frac{\overline{(P4-P1)_t} - \overline{(P4-P1)_{t=0}}}{\overline{(P4-P1)_{t=0}}}\ [\text{mm/mm}]$$

$$\Delta R_t = \measuredangle(P1,P2,P3)_t - \measuredangle(P1,P2,P3)_{t=0}\ [^\circ]$$

**Fig. 4.** Locations of tracked features during the seismic test, including determination of distances D (left), strains T, M (center) and rotations R (right).

sentative and interesting observations identified in this research are marked. Detachments *D* between the timber frame and the masonry were monitored by measuring distances between two points and were expressed directly in millimetres. Rotations *R* between members of the timber frame were analysed by measuring the change of the angle between two segments having one common point. Four point-polylines defined polygonal fields inscribing 4 portions of the framed wall: two lateral portions, one attached to the piston (1 in Fig. 4) and the other on the opposite side of the window opening (2 in Fig. 4); and two portions above and below the window opening (3 and 4 in Fig. 4, respectively). The four point-polylines were used to observe and describe the overall behaviour of the framing elements *T* and the masonry infill *M*.

## 4. Results and discussion

### 4.1. Capacity curve

Information on the post-elastic displacements in cycle tests is typically obtained from the capacity curve in the form of envelope curve of the force-deformation diagrams. The curve in Fig. 5 shows a pseudo-plastic phase starting after the 7 mm displacement cycling, with a stiffness drop after the 60 mm cycle, and force $F_{max}$ equal to 103.6 kN (drift 2%).

The recorded ductility value ($\mu = V_u/V_y$) was of 7.6 (positive direction). Therefore, according to Eurocode 8, the specimen emphasized a considerable ductile response.

The backbone curve showed a terminal softening branch in the positive direction and a slow regaining of strength in the last steps of the loading. A moderate pinching can be observed in the load-displacement curve for 60–80 mm displacement in both directions. The pinching phenomenon may be attributed to the detachment of the masonry infill from the frame and the generation of a gap during the reversed cyclic loading increase. It resulted in a decrease of the equivalent viscous damping ratio (*EVDR*) between 6% and 10%. This phenomenon is further analyzed in the following sections through the application of the proposed image-based tracking method.

### 4.2. Strain

After the cycles with a displacement of about 7 mm, the wall experienced an asynchronous motion and generation of 4 sub-panels, as presented in Fig. 4. It included two vertical sub-panels (1 and 2) at the two sides of the window opening, a horizontal sub-panel (3) the spandrel and a lower masonry block (4) devoid of internal timber framing [22].

Figs. 6–9 show the calculated strain values of the edges of the polygonal bases in each wall sub-panel during the loading cycles. The strain cycles in the right edge of the timber frame (post) and in the masonry were synchronous and increasing for increasing values of set displacement (Fig. 6, sub-panel 1). At the internal post (left) of sub-panel 1, an intermediate strain cycle occurred during pushing (from the first cycle of 40 mm displacement), while the masonry exhibited positive strain values during pulling. Moreover, values of strain in the left post are mainly negative for the masonry, while they are all in the positive field in the frame from the first 60 mm cycle. Absolute strain values, measured at the external post of sub-panel 1 for the 80 mm cycles are 400% higher than those measured at the internal post. In the right post, positive values (corresponding to the pulling action of the actuator) are higher than negative values, and for each cycle, values in the frame are higher than in the masonry.

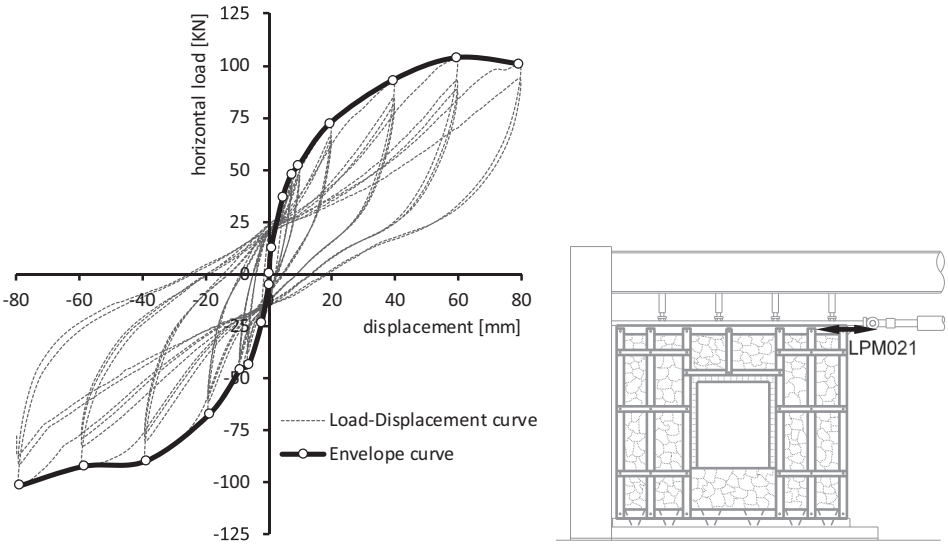


**Fig. 5.** Capacity curve of the Borbone system specimen subjected to a quasi-static cyclic test.

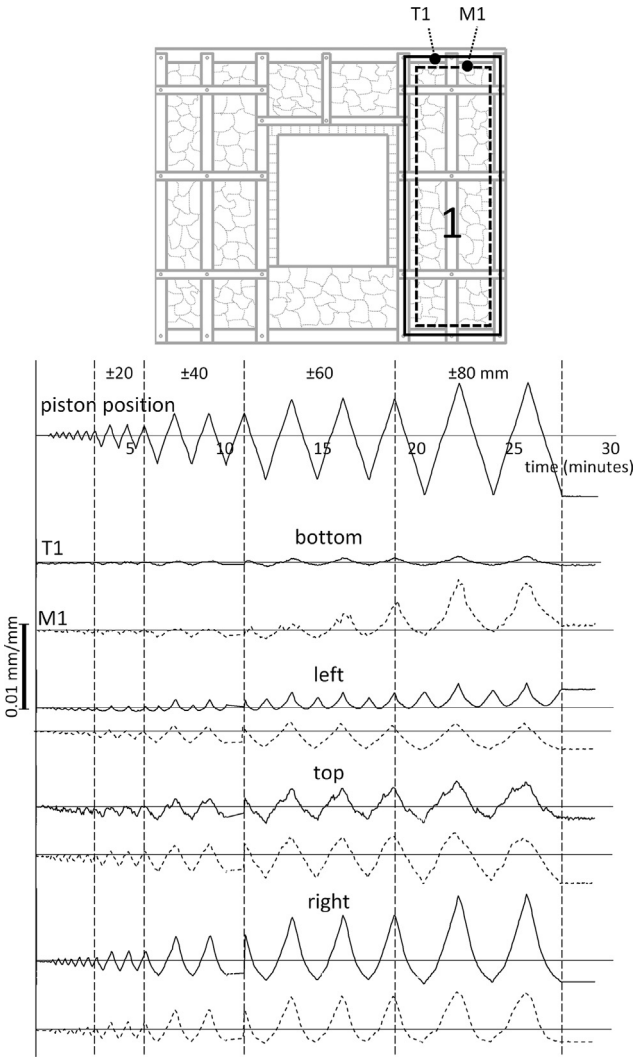


**Fig. 6.** Strains on the right column (1) in the timber frame (continuous line) and masonry (dashed line).

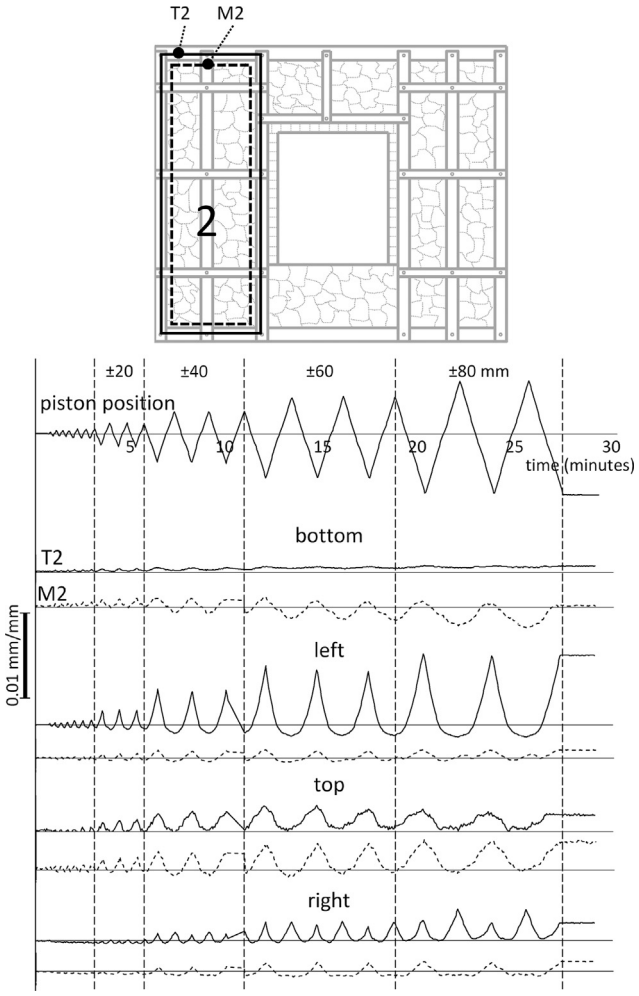


**Fig. 7.** Strains on the left column (2) in the timber frame (continuous line) and masonry (dashed line).

The situation observed in sub-panel 1 was nearly inverted in sub-panel 2 (Fig. 7). The timber frame's external post exhibited strain values 200% to 600% higher than the masonry.

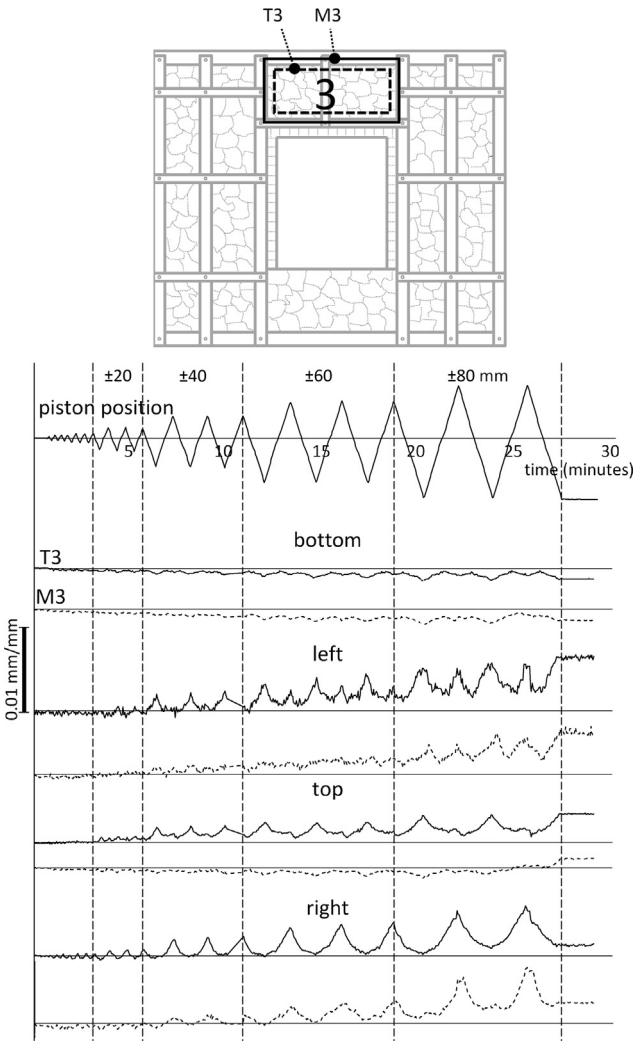


**Fig. 8.** Strains on the spandrel (3) in the timber frame (continuous line) and masonry (dashed line).

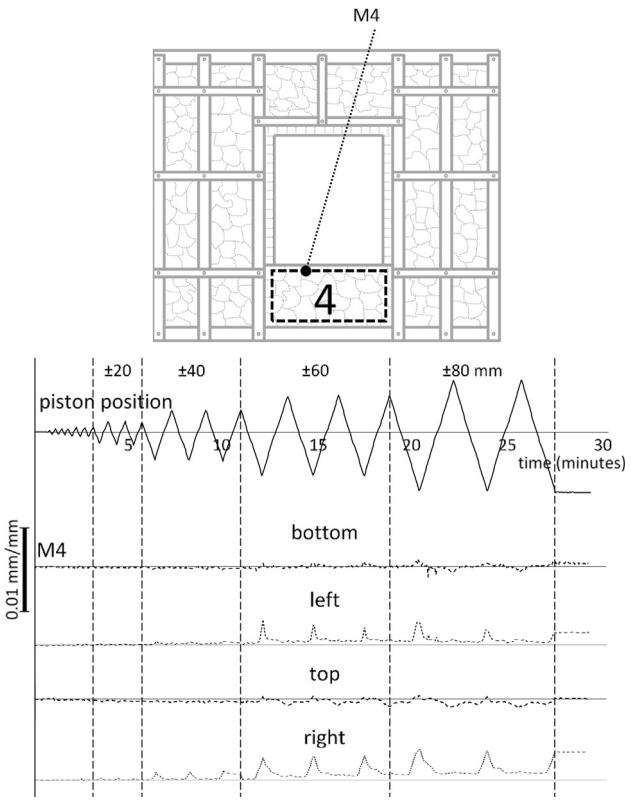


**Fig. 9.** Strains on the bottom wall (4) in the masonry (dashed line).

Strain in the horizontal segments of the polyline inscribing sub-panel 1 (Fig. 6) was concordant in the masonry and in the frame with almost correspondent values in the upper segments, except for the final six negative cycles. Instead, values at the masonry close to the bottom segment started to increase in the last four pulling cycles, reaching a difference of 800% from values recorded in the frame in the last cycle.

A similar behavior was observed in sub-panel 2 (Fig. 7). In this case, the lower horizontal timber member did not show strains during the cycles, while the masonry portion exhibited increasing negative strain values during pulling.

The external posts of both lateral sub-panels 1 and 2, exhibited higher strain rates since they were unrestrained on one side. The internal posts of the piers in sub-panels 1 and 2 behaved unexpectedly (i.e., intermediate peaks were observed). This was because the movements of the two lateral sub-panels were partially restrained by the unframed masonry portion (sub-panel 4). While both, the frame and the masonry, followed the movement of the actuator in the direction of the unrestrained side (pushing for sub-panel 1 and pulling for sub-panel 2), the strain in the frame was the inverse of the actuator action towards the restrained direction, while the masonry followed the actuator. This can be explained by the presence of the sub-panel 4, which pushed the post back in the opposite direction of the actuator.

At the lower horizontal edge of both sub-panel 1 and 2, the timber sill plate, which was connected to the testing frame base, did not exhibit significant displacement. However, the presence of increasing strains in the infill occurred during the last 60 mm cycle indicated a crack development.

In sub-panel 1, positive to null strains, induced by pulling and pushing respectively, indicated the presence of two separated portions of the infill, which moved to fill a formed gap before to move together. An analogous behavior was observed in sub-panel 2, but for the opposite direction of the action.

In the spandrel (sub-panel 3 – Fig. 8), increasing strain values were observed on both vertical edges. The strain diagram was approximately flat for the bottom edge of the spandrel both in the timber and masonry portions. This was likely because this portion of the wall, joined at the extremes to the internal posts, followed the movement of the lateral sub-panels through rigid rotations at the joint with no development of strains. To prove this assumption, further analysis of the rotation at this connection follows in next sections of this manuscript (Rotations) and Fig. 11. The timber element at the top edge of the spandrel exhibited a cyclic response, while the corresponding masonry portion did not show significant strains. This was caused by an almost immediate detachment of the masonry block from the top plate, which caused the whole infill portion to rest on the header above the opening. In contrast, the timber portion, which was part of the top plate and was a continuous member for the entire width of the wall, exhibited comparable behavior in each of three sub-panels (1, 2, 3).

Sub-panel 4 (Fig. 9) consisted only of masonry resting on the sill plate. It received the action of the actuator indirectly through the pushing and pulling exerted by the lateral piers (sub-panels 1, 2). The top and bottom edges of sub-panel 4 did not exhibit any strain cycles. While the bottom portion remained inert on the sill plate, the upper portion of the masonry translated rigidly due to the action transmitted by the piers. The two lateral edges exhibited

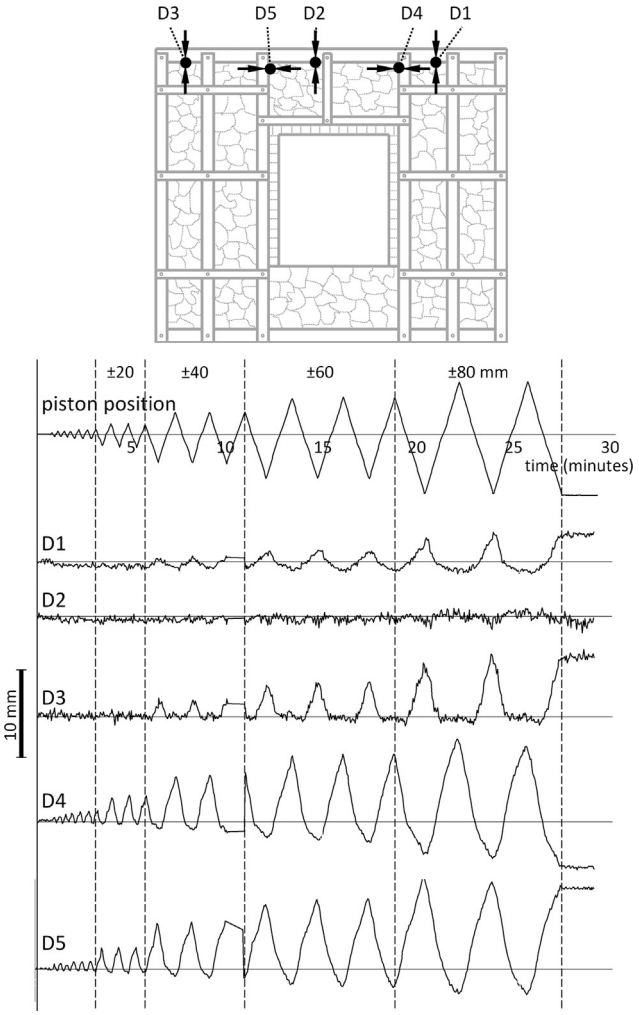


**Fig. 10.** Vertical and horizontal distances of openings describing the detachment of the masonry from the timber frame.

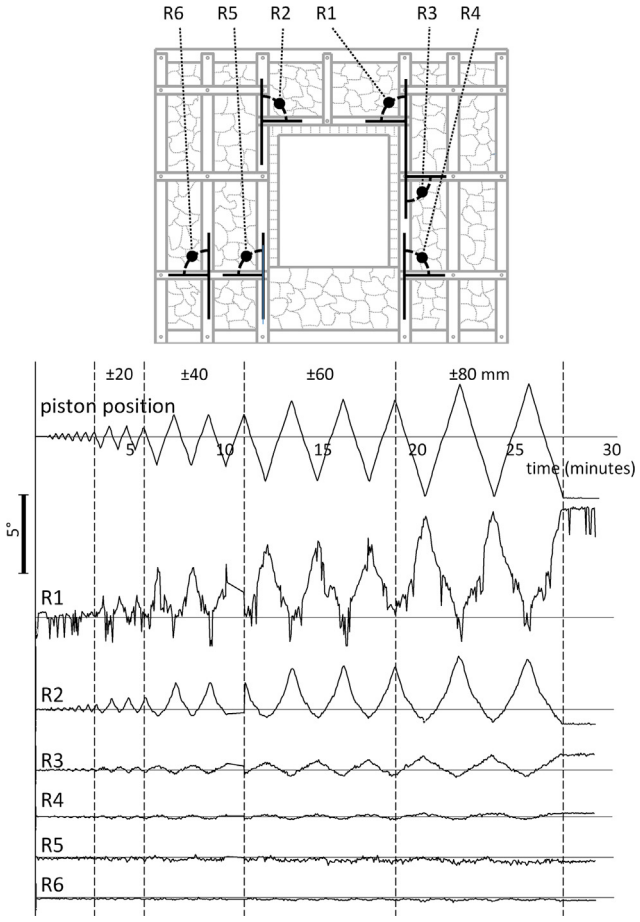


**Fig. 11.** Local rotations of the timber frame joints.

concordant and higher strain values during pushing. This was due to local phenomena, i.e., development of cracks, caused by the fact that the unreinforced masonry did not behave monolithically, but instead separated in sub-blocks which moved rigidly during cycling. This is particularly evident in the sudden change of values in both the left and right edges, occurring during the first cycle of 60 mm in pushing. In our experimental setup, this phenomenon was expressed as strain in the entire sub-panel, rather than in individual sub-blocks which moved separately and caused the effect.

As a general observation, the strains charted in the panel diagrams were not coincident between the timber frame and the masonry infill, even when they show a similar trend (Fig. 6, right and top; Fig. 7, top portion; Fig. 8, right edge). This observation leads us to deduce that the masonry infill has become detached from the timber frame. In this case, the motion in the infill followed the timber frame but with some delay, since part of the energy transmitted by the actuator was used to fill the gap. Action was then transmitted to the rest of the masonry after the initial gap was filled.

As the strain curves of both portions of the sub-panel did not follow the same trend (there was a sudden variation of the strain values disproportional to the cycle change), a crack likely developed in the masonry. This caused the infill to not behave as a singular element, but rather as a composite of independent blocks, as in the case of sub-panel 4.

### 4.3. Infill detachment

In Fig. 10, locations are marked (*D1, D2, D3, D4,* and *D5*) where the distance between two points was monitored. In each set of points, one was on the timber frame and the other was on the masonry infill. The displacement curves for each marked set of points charts the change in distance between the paired points over time. These observations reveal and characterise the separation between the timber frame and the masonry infill. *D1*, *D2*, and *D3* describe local detachments at the top plate between the timber frame and the underlying masonry infill. Values in *D1*, *D2*, and *D3* are comparable until the first 40 mm displacement cycle. This trend continued throughout the test in the pulling portions of the cycles. However, in pushing portions of the cycles the behaviour at each location became divergent beginning with the first 40 mm displacement cycle, as shifts in the displacement amplitude began to vary between *D1*, *D2*, and *D3*. This phenomenon progressed steadily with each increase in the actuator displacement amplitude.

Behaviour in *D2* is likely caused by the indirect motion applied at this location; the spandrel receives its action indirectly from the lateral sub-panels 1 and 2 on either side of it.

Distance values at locations *D5* and *D4* indicate detachments that occurred between the timber posts and the masonry infill of the spandrel (Fig. 10). *D5* and *D4* had similar separation magnitudes, but opposite separation directions. The generated gaps were partially (and alternatively) recovered, depending on the direction of the action. The detachments observed were because the timber frame followed the action of the actuator but the infill was more

inert. The vertical detachments in sub-panels 1 and 2, as observed after the first cycle of 40 mm, were likely due to the local embedding and bending of the pyramidal nails at the joints connecting the top plate and internal posts.

### 4.4. Rotations

3-point "virtual transducers" connecting two members of the timber frame at selected nodes describe local rotations at the timber joints (Fig. 11). The rotation in node *R1* was approximately constant during pushing, while it increased proportionally to the action of the actuator during pulling. The behavior was analogous in node *R2*, but the rotational direction was reversed. The rotation directions indicate the rotation of the spandrel as it transfered the action of the piston from sub-panel 1 to sub panel 2. Rotation measured in two aligned nodes on the internal posts in sub-panel 1 (*R1* and *R3*) differed by about 500%, with *R3* (node between the post and the intermediate horizontal member in the pier) exhibiting the lower values. The rotation observed at the joints between the spandrel and sub-panels 1 and 2 explains the negligible strain values in the horizontal members of the sub-panel 3 (Fig. 9).

Rotations in the lower points (*R4* and *R5*) within sub-panels 1 and 2 as well as in *R6* (internal lower node in the sub-panel 2, but opposite to the actuator) were minimal.

The trends in rotation values (as reported in Fig. 11) suggest that the two lateral sub-panels 1 and 2 started to deflect at approximately 70 cm above the sill plate, which corresponds to the height of the wall section below the window opening, due to sub-panel 4 stiffening the bottom part of the piers.

Summarizing, it was found that the side parts of the wall (columns 1 and 2) deforms in the same manner, with the outer sides the most pronounced. The movements of the bottom wall (4) were minor, while the upper part (spandrel 3) correlates with the movements of the neighboring wall components. Horizontal detachments occurs in upper regions of the wall, especially in columns and spandrel. Vertical detachments were minor, and were detected mostly on sides.

## 5. Conclusions

The image-based tracking method developed in this study allowed analysis of local phenomena and damage progression in an historical timber frame system. This type of observation is important for the design of rigorous strengthening or repair interventions.

When considering the conclusions about the effectiveness of the proposed image tracking method, it is important to recall that:

(a) this analysis is complementary and not alternative to "traditional" studies that rely on readings from LVDTs;
(b) the final cycle of this experiment was not completed and does not allow proper evaluation of residual phenomena (i.e., distances, strains, rotations);
(c) the analytical method used has some inherent limitations (i.e., image distortion and limited resolution of the analysed sequence of images, inability to analyse out-of-plane behaviour, among the others).

In the studied historical construction, the masonry provides the main load bearing system under static forces, while the timber frame provides the bulk of the seismic capacity of the system through its tension resistance. The system is effective for moderate seismic loads as it restrains the masonry [23]. The masonry has a strategic role of limiting excessive deformations of the timber structure (i.e., mainly by bracing the wood frame and by increasing the energy dissipation through friction development after cracks).

It is clear that any structural test has to strictly follow established standards and protocols in order to allow comparison with results of similar tests. However, the amount of information available as the output of such test is sometimes limited and usually includes series of time resolved forces and displacements. Data obtained from LVDT in typical test configurations can be sometimes insufficient to analyze all unforeseen, local phenomena. On the other hand, photographic (or video) documentation of the cycling loading tests is a simple procedure providing valuable data for a complementary analysis without interfering with the defined protocols. Considering the above, we developed an image-based tracking method for the specific needs of this study. Nevertheless, the method may have broader applications. As it is a prototype, the numerical solutions are a pilot or proof of concept. For that reason, the image tracking method at this stage of development cannot substitute LVDT data acquisition, but rather offer a highly useful and simple tool, providing unlimited possibilities for supplementary studies and tailored structural analyses.

The tested construction system responds appropriately to cyclic loading confirming the positive seismic behavior showed in previous earthquakes (i.e., those that occurred in 1905 and 1908 [2]).

Modern seismic engineering practices recommend application of capacity design criteria to ensure that a building undergoes controlled ductile behavior. This involves designing the structure to allow concentration of inelastic behavior in specific, predictable locations. In that case, the demands on the portions of the structure designed to remain essentially elastic during an earthquake are limited. This can be achieved in timber engineering by relying on the ductile behavior of the joints, while timber elements are over-dimensioned and can be loaded within the elastic limit.

Throughout the entire test, all the members continued acting in the pseudo-elastic field showing no rupture or plastic deformations and dissipated seismic energy by means of friction [24]. According to the analysis conducted with this study, it is possible to deduce that plastic deformations and local damage occurred in some joints, for instance those connecting the posts with the top plate, the spandrel, and the sill plate. Rotation actions caused the plastic compression of wood surface at the contact zone of both jointed members. This took place after the relative movement exceeded the initial gap between the two contact surfaces of the perpendicular joint.

Damage observed in the masonry infill consisted of detachments from the frame, internal rupture and separation of blocks within the masonry along the mortar joints. This behavior indicated an effective seismic response since damage of the masonry infill precedes any damage in the timber frame.

It is important to note that stone or brick expulsion during progressive damage of the infill, even if not critical from a structural point of view, can cause injury to people and damage to other objects. Therefore, while damage in the masonry infill can be easily repaired after a seismic event [25], some provision should be adopted in restoration interventions to avoid fragment expulsions.

New interventions should preserve the integrity and authenticity of this traditional system [26,27]. Accordingly, solutions should be adopted so that damage can be concentrated in the new integration/strengthening element, thus preserving the original structure.

## Declaration of interests

The authors declared that there is no conflict of interest.

## Acknowledgements

The authors would like to acknowledge Prof. A. Ceccotti and Dr. A. Polastri, for their leading roles during the experimental testing of the wall, Dr. M. Negri and Dr. M. Fellin, for sharing the image data. The staff of the Mechanical Testing Laboratory at CNR-IVALSA is acknowledged for their contribution in the experimental campaign. The authors would like to thank Dr. Paolo Grossi and Dr. Mike Burnard for their thoughtful comments.

Jakub and Anna Sandak gratefully acknowledge the European Commission for funding the InnoRenew CoE project (Grant Agreement #739574) under the Horizon2020 Widespread-Teaming program and BIO4ever project (RBSI14Y7Y4) funded within a call SIR by MIUR.

## References

[1] N. Ruggieri, The borbone "Istruzioni per gli ingegnieri" a historical code for earthquake-resistant constructions, Int. J. Architect. Heritage 11 (2) (2016) 292–304.
[2] N. Ruggieri, G. Tampone, R. Zinno, Typical Failures, Seismic Behavior and Safety of the "Bourbon system" with Timber Framing, Advanced Materials ResearchAdvanced Materials Research, vol. 778, Trans Tech Publications, Switzerland, 2013, pp. 58–65.
[3] Ruggieri, N., Tampone, G., Zinno, R. (2015). In-plane vs Out-of-plane "Behaviour" of an Italian Timber Framed System: the Borbone Constructive System. Historical Analysis and Experimental Evaluation, International Journal of Architectural Heritage, 9:6, pp. 696-711
[4] S. Santos, Tests of Pombalino walls [in Portuguese]. Lisbon, Portugal: Laboratório Nacional de Engenharia Civil (LNEC). Nota Técnica No 15/97–NCE, 1997
[5] G. Vasconcelos, E. Poletti, Seismic behaviour of traditional half timbered walls: cyclic tests and strengthening solutions, in: J. Jasienko (Ed.), Proceedings of International Conference Structural Analysis of Historical Constructions, 2012.
[6] A. Gonçalves, P. Candeias, L. Guerreiro, J. Ferreira, A. Costa, Characterization of timber masonry walls with dynamic tests, in: H. Cruz, J. Saporiti Machado, A. Campos Costa, P. Xavier Candeias, N. Ruggieri, J. Manuel Catarino (Eds.), Historical Earthquake-Resistant Timber Frames in the Mediterranean Area, second ed., Springer International Publishing, Switzerland, 2016, pp. 299–309.
[7] H. Krawinkler, F. Parisi, L. Ibarra, A. Ayoub, R. Medina, Development of a testing protocol for wood frame structures Report W-02 covering Task 1.3.2, CUREE/Caltech Wood frame Project, Consortium of Universities for Research in Earthquake Engineering (CUREE), Richmond, CA, USA, 2001.
[8] A. Dutu, H. Sakata, Y. Yamazaki, Comparison between different types of connections and their influence on timber frames with masonry infill structures' seismic behaviour, 16th World Conference on Earthquake, 16WCEE 2017, Santiago Chile, 2017.
[9] Q. Ali, T. Schacher, M. Ashraf, B. Alam, A. Naeem, N. Ahmad, M. Umar, In-plane behaviour of Dhajji-Dewari structural system (wooden braced frame with masonry infill), Earthq. Spectra 28 (3) (2012) 835–858.
[10] N. Quinn, D. D'Ayala, D. Moore, Experimental testing and numerical analyses of Quincha under lateral loading, in: J. Jasienko (Ed.), Proceedings of International Conference Structural Analysis of Historical Constructions, Wroclaw, Poland, 2012.
[11] Y.D. Aktas, U. Akyüz, A. Türer, B. Erdil, N. Sahin Güçhan, Seismic resistance evaluation of traditional Ottoman timber-frame himis houses: Frame loadings and material tests, Earthq. Spectra 30 (4) (2012) 1711–1732.
[12] P. Ceccotti, M. Faccio, P Simeone Nart, Seismic behaviour of historic timber frame buildings in the Italian dolomites, Proceedings of 15th international symposium ICOMOS international wood committee, Istanbul and Rize, 2006.
[13] Y. Sieffert, F. Vieux-Champagne, S. Grange, P. Garnier, J.C. Duccini, L. Daudeville, Traditional timber-framed infill structure experimentation with four scales analysis (to connection from a house scale), in: H. Cruz, J. Saporiti Machado, A. Campos Costa, P. Xavier Candeias, N. Ruggieri, J. Manuel Catarino (Eds.), Historical Earthquake-Resistant Timber Frames in the Mediterranean Area, second edition., Springer International Publishing, Switzerland, 2016, pp. 287–297.
[14] M. Baratta, La catastrofe sismica calabro messinese, Società Geografica Italiana, Roma, 1908 (in Italian).
[15] http://www.protezionecivile.tn.it.
[16] M. Brunetti, Il futuro: progettare con il legno, Caratteristiche antisismiche, Restauro, nuove costruzioni, Università della Calabria, 2012. 10th July, 2012.
[17] S.L. Kelton, S.R. Arwade, A.J. Lutenegger, Variability of the mechanical properties of wrought iron from historic American truss bridges, J. Mater. Civil Eng., ASCE (2011) 638–647.
[18] EN 1991-1-1, Eurocode 1: Actions on Structures, CEN European Committee for Standardization, Brussels, Belgium, 2002.
[19] CEN EN 12512, Timber Structures – Test Methods – Cycling Testing of Joints Made with Mechanical Fasteners, CEN European Committee for Standardization, Brussels, Belgium, 2006.
[20] EN 1998-1, Eurocode 8: Design of Structures for Earthquake Resistance, CEN European Committee for Standardization, Brussels, Belgium, 2004.
[21] E. Poletti, G. Vasconcelos, Seismic behavior of traditional timber frame walls: experimental results on unreinforced walls, Bull. Earthq. Eng. 13 (3) (2015) 885–916.
[22] J. Sandak, N. Ruggieri, M. Riggio, M. Fellin, A. Sandak, A. Polastri, A. Ceccotti, An Italian historic timber framed wall: damage progression through DIC analysis, in: J. Jasienko, T. Nowak (Eds.), Structural Health Assessment of Timber Structures, Wroclaw – Poland, 2015 (ISBN 978-83-7125-255-6).
[23] S. Di Pasquale, U. Tonietti, G. Tempesta, Architettura e terremoti, Pratiche (1986).
[24] S. Galassi, N. Ruggieri, G. Tempesta, Seismic performance evaluation of timber-framed masonry walls. Experimental tests and numerical modelling, in: N. Ruggieri, G. Tampone, R. Zinno (Eds.), Historical Earthquake-Resistant Timber Frames in the Mediterranean Area, Springer International Publishing, 2015.
[25] M. Paradiso, S. Galassi, A. Borri, D. Sinicropi, Reticolatus: an innovative reinforcement for irregular masonry. A numeric model, in P.J.S. Cruz (ed.), Structures and Architecture: Concepts, Applications and Challenges, Proc. of 2nd International Conference on Structure & Architecture ICSA 2013, Guimaraes, Portugal, 2013
[26] ICOMOS International Wood Committee, Principles for the preservation of historic timber buildings, 14th Symposium in Patzcuaro Michoacan, Mexico November 10–14, 2003, 2003.
[27] M. Piazza, M. Riggio, Typological and structural authenticity in reconstruction: the timber roofs of church of the Pieve in Cavalese, Italy, Int. J. Architect. Herit. 1 (60–81) (2007) 2007.